



I S A V

**Journal of Theoretical and Applied
Vibration and Acoustics**

journal homepage: <http://tava.isav.ir>



Renovation of modified Biot's theory for modeling of the nanocomposite porous materials: A theoretical and experimental acoustical study

Mohamad Mirmasoumi ^a, Abolfazl Hasani Baferani ^{b,*}, Abdolreza Ohadi ^a

^a Acoustics Research Lab., Department of Mechanical Engineering, Amirkabir University of Technology, Tehran, Iran.

^b Department of Mechanical Engineering, Tafresh University, Tafresh, Iran.

Research Article

ARTICLE INFO

Article history:

Received 11 February 2025

Received in revised form
24 August 2025

Accepted 30 August 2025

Available online 28 November
2025

Keywords:

Acoustic

Modified Biot's theory

Nonlocal

Nanocomposite foam

Transfer matrix method

ABSTRACT

In this paper, the modified Biot's theory is revised to predict the acoustic performance of nanocomposite porous materials more accurately, based on the nonlocal elasticity theory. The governing equations are derived for a transversely isotropic porous medium. The transfer matrix method is developed for the first time to obtain the absorption coefficient by introducing two non-local parameters, solid and fluid, to consider non-local effects. Subsequently, several nanocomposite foams are produced by various multiwall carbon nanotubes to validate the theoretical results. Different mechanical, acoustical, and non-acoustical properties of produced samples have been experimentally measured or calculated. Sound absorption for various solid and fluid nonlocal parameters is presented and compared with the corresponding absorption coefficient experimentally obtained from the impedance tube test. The obtained results show that by ignoring the fluid nonlocal effect, the experimental results agree well with the theoretical predictions based on modified Biot's theory in wave propagation for large values of the solid nonlocal parameters.

© 2025 Iranian Society of Acoustics and Vibration, All rights reserved.

* Corresponding author.

E-mail address: baferani@tafreshu.ac.ir (A. Hasani Baferani)

<http://dx.doi.org/10.22064/tava.2025.2053152.1261>

1. Introduction

Nanocomposites are materials with several different phases and have attracted significant interest from researchers and manufacturers due to their enhanced mechanical, thermal, acoustic, and electrical properties. Using carbon nanotubes to produce nanocomposite foam affects the porous material's fluid and solid phases. Alternatively, carbon nanotubes in the production of nanocomposite foam cause nucleation, leading to changes in the size and number of cells. Consequently, various parameters, such as thermal characteristic lengths, viscous characteristic lengths, tortuosity, and porosity, will be influenced.

Furthermore, carbon nanotubes in the production process cause the cells to become more closed, increasing the flow resistivity of the produced nanocomposite sample. The mentioned factors in each of the viscous and thermal damping factors change the properties of the produced nanocomposite samples. Another effect is the presence of carbon nanotubes in the solid phase of the nanocomposite foam. Carbon nanotubes in different polymer segments of the nanocomposite sample form a stronger bond between the carbon nanotubes and the polymeric segments and naturally reinforce the microstructure. The effect of this phase on the outcomes of carbon nanotubes is evident in structural damping and typically manifests at higher frequencies.

Many studies have focused on modeling nanocomposite foams [1-4] and investigated the effect of carbon nanotubes on the various properties of producing nanocomposite samples [5-10]. To consider the effect of carbon nanotubes in the solid phase, a more accurate solution is required. There are different continuous medium theories to model the macroscopic and microscopic behavior of other materials. However, a solution to the governing equations of nanocomposites to consider the effect of microstructure on the solid phase is the Eringen theory. Eringen [11] presented the nonlocal elasticity theory to develop continuous medium theories for predicting the behavior of various materials at the nanoscale, taking the effects of the length parameter into account [12]. The assumption of this theory is to consider the acting forces around the body particles. In other words, it expresses the stress at a point in the body, depending on the strains at all points of the continuum media [13-17].

Chakrabarty [18] described the negative dispersion of wave propagation in cancellous bone using modified Biot's theory. Some deviations in the wave propagation characteristics have occurred due to the consideration of the non-local effects of the fluid. Wave propagation characteristics in porous materials saturated by fluid were investigated by Tong et al. [19] based on modified Biot's theory. They used this model to account for nonlocal effects in both the solid and fluid phases; however, only the solid nonlocal effects were included, while the fluid nonlocal effects were omitted. Baferani and Ohadi [20] presented the modified Biot equations for the first time to model wave propagation in isotropic nanocomposite porous materials. They applied the same values of nonlocal parameters for solid and fluid phases and solved the governing equations using the potential function method. They demonstrated that the results of the Biot theory align with those of the modified Biot theory when the nonlocal parameters are small. Tong et al. [21] applied the modified Biot's theory to investigate the nonlocal parameter effect on Rayleigh wave propagation in porous materials saturated by fluid. They investigated the dynamic effect of a ring load on a cylindrical structure embedded in a saturated porous medium theoretically using Biot's nonlocal theory. They obtained general solutions for displacements, stresses, and pore pressure using the Fourier transform [22].

Menon and Song [23] presented a stable computational nonlocal poro-mechanics model that can be used to analyze dynamically saturated porous media. In this method, the nonlocal formulations of skeleton strain energy and fluid flow dissipation energy correspond to their local formulations. Ding et al. [24] investigated the determination of the nonlocal parameter and scale factor, as well as how grain size, porosity, and grain size distribution affect these size parameters. Based on the presented results, the value range and influence factors of these two critical parameters introduced in strain gradient nonlocal Biot's theory are determined. Their findings are of great significance for popularizing and applying this theory to engineering practices. Xenon [25] investigated the development, calibration, and numerical implementation of a novel fully explicit isotropic, rate-independent, elastic-plastic model for porous metallic materials. They presented different methods and numerical procedures.

In the majority of the studies reviewed above, the modified Biot's theory has been used to predict the acoustic performance of isotropic porous materials with a particular nonlocal parameter for solid and fluid phases; however, the absorption coefficients of these materials have not been evaluated in the presence or absence of the nonlocal parameter of the fluid phase. Additionally, they should be compared with the experimental results. Furthermore, previous research has not used the transfer matrix method to solve the modified Biot theory.

The present study is devoted to deriving a modified Biot's theory by combining Biot's theory [26] and nonlocal elasticity theory [4] to model the expected wave propagation in isotropic or transversely isotropic nanocomposite porous layers. In this paper, the solid and fluid nonlocal parameters are introduced to consider the nonlocal effects of stress, and Biot's equations are modified by the nonlocal elasticity theory. To solve the equations, the transfer matrix method is developed for the first time. In addition, several foam nanocomposite samples are produced. Meanwhile, the non-acoustic and mechanical characteristics of the produced samples are measured, and the experimental and theoretical results are compared.

2. Modified Biot's theory

Eringen's nonlocal elastic theory [12, 13, 15, 16] is one of the most widely used approaches to consider length effects in continuous models. Eringen's nonlocal theory, which utilizes classical elasticity, does not apply to molecular dynamics. It also has a length parameter that can significantly influence the modeling of nanostructures. Biot's equations should be modified by the nonlocal elasticity theory to obtain the governing equations. Therefore, the Biot equations [27] are rewritten as follows

$$\sigma_{ij,j}^{t(nl)} = \rho \ddot{u}_i^s + \rho_0 \ddot{w}_i \quad (1)$$

$$-p_{,i}^{(nl)} = \rho_0 \ddot{u}_i^s + C_i \ddot{w}_i \quad (2)$$

where the $\sigma_{ij,j}^{t(nl)}$ represents the nonlocal total stress tensor and $p^{(nl)}$ is the nonlocal acoustic pressure. Additionally, a dot above each parameter denotes partial differentiation concerning $(\dot{\quad}) = d()/dt$. The subscripts i and j indicate the derivation of parameters in terms of x and y , respectively. In addition, $\rho = \rho_1 + \phi \rho_0$ is the total density of the porous media, ρ_1 represents the

bulk density, ρ_0 is the fluid density, u_i^s denotes the components of solid-phase displacement, $w_i = \phi(u_i^f - u_i^s)$ are the components of fluid-discharge or relative displacement, u_i^f are the components of fluid phase displacement, $\tilde{\rho}_{12}^i$ and $\tilde{\rho}_{22}^i$ are the dynamical coefficients given as follows [28]

$$\tilde{\rho}_{22}^i = \phi\rho_0 - \tilde{\rho}_{12}^i \quad (3)$$

$$\tilde{\rho}_{12}^i = \phi\rho_0(1 - \tilde{\alpha}_\infty^i) \quad (4)$$

where ϕ represents porosity and $\tilde{\alpha}_\infty^i$ is the dynamic tortuosity of Johnson's model [29] to consider the effects of porous media viscosity. Since there are two solid and fluid phases in a porous medium, μ_s and μ_f are regarded as a nonlocal parameter of solid and fluid phases, respectively. The terms of $1 - \mu_s\nabla^2$ and $1 - \mu_f\nabla^2$ are applied on both sides of Equations (1) and (2), respectively. The nonlocal effects of solid and fluid phases are imposed simultaneously, yielding the Biot equations as follows:

$$\sigma_{ij,j}^{(l)} = (1 - \mu_s\nabla^2)(\rho\ddot{u}_i^s + \rho_0\ddot{w}_i) \quad (5)$$

$$-p_{,i}^{(l)} = (1 - \mu_f\nabla^2)(\rho_0\ddot{u}_i^s + C_i\ddot{w}_i) \quad (6)$$

Also, by assuming the solid phase and fluid-discharge displacements in terms of a frequency-dependent exponential function, modified Biot's equations in terms of the frequency are written as follows:

$$\sigma_{ij,j}^{(l)} = -\omega^2(1 - \mu_s\nabla^2)(\rho u_i^s + \rho_0 w_i) \quad (7)$$

$$-p_{,i}^{(l)} = -\omega^2(1 - \mu_f\nabla^2)(\rho_0 u_i^s + C_i w_i) \quad (8)$$

Considering the z -axis as the axis of the material's symmetry, the x and y axes will be orthogonal in the symmetry plane. Also, the fluid bulk modulus, \tilde{K}_{eq} , is calculated based on the Champoux-Allard model [30]. In this section, the modified Biot equations have been extended by considering the non-local parameters of the solid phase μ_s and fluid phase μ_f , independently. An attempt was made to improve the modified Biot theory by considering different values of non-local parameters of solid and fluid.

3. The transfer matrix method

To investigate the acoustic behavior of nanocomposite porous materials based on modified Biot's theory, specific solution methods are required to solve the governing equations. The modified Biot equations are typically solved only for isotropic porous materials using analytical methods, which are very complex and practically inapplicable for transversely isotropic porous media. The transfer matrix method can be applied here to solve these equations for the first time, considering both the solid and fluid phase nonlocal effects.

The transfer matrix method should be applied to the solid nonlocal effect in all directions and the fluid nonlocal effect in the z -axis direction. Since the wave propagation is perpendicular to the layer's surface, it doesn't change the final solution. Thus, by expanding Equations (7) and (8) and ignoring the nonlocal effect of the fluid phase in the x -axis and y -axis direction, they are rewritten as follows:

$$\frac{\partial \sigma_{xx}^{(l)}}{\partial x} + \frac{\partial \sigma_{xy}^{(l)}}{\partial y} + \frac{\partial \sigma_{xz}^{(l)}}{\partial z} = -\omega^2(1 - \mu_s \nabla^2)(\rho u_x^s + \rho_f w_x) \quad (9)$$

$$\frac{\partial \sigma_{yx}^{(l)}}{\partial x} + \frac{\partial \sigma_{yy}^{(l)}}{\partial y} + \frac{\partial \sigma_{yz}^{(l)}}{\partial z} = -\omega^2(1 - \mu_s \nabla^2)(\rho u_y^s + \rho_f w_y) \quad (10)$$

$$\frac{\partial \sigma_{zx}^{(l)}}{\partial x} + \frac{\partial \sigma_{zy}^{(l)}}{\partial y} + \frac{\partial \sigma_{zz}^{(l)}}{\partial z} = -\omega^2(1 - \mu_s \nabla^2)(\rho u_z^s + \rho_f w_z) \quad (11)$$

$$-\frac{\partial p^{(l)}}{\partial x} = -\omega^2(\rho_f u_x^s + C_x w_x) \quad (12)$$

$$-\frac{\partial p^{(l)}}{\partial y} = -\omega^2(\rho_f u_y^s + C_y w_y) \quad (13)$$

$$-\frac{\partial p^{(l)}}{\partial z} = -\omega^2(1 - \mu_f \nabla^2)(\rho_f u_z^s + C_z w_z) \quad (14)$$

One may consider a normal plane wave propagating in the xz -plane in a nanocomposite porous layer with infinite lateral dimensions connected to a rigid, impermeable backing. As shown in Figure 1, a part of this wave is absorbed (p_1), while a part is reflected as (p_2).

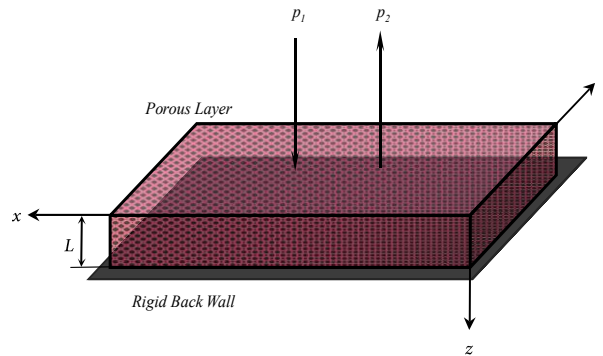


Fig.1. Normal wave propagation in a nanocomposite porous layer with infinite lateral dimensions connected to a rigid, impermeable backing.

Therefore, the governing equations can be solved by considering boundary conditions in the free air close to the upper face of the layer and behind it. The z -axis is assumed to be the axis of rotational symmetry, and the x -axis in the meridian plane is considered perpendicular to the z -axis. A harmonic plane wave with the slowness components $q_x = 1/C_0$ in the x -direction, $q_y = 0$ in the y -direction, and $q_z = q$ in the z -direction, propagates in a nanocomposite porous layer [28]. Thus, the displacement components are derived from Equations (15) and (16).

$$u_i^s = a_i \exp(j\omega(t - q_x x - q_y y - q_z z)), i = x, y, z \quad (15)$$

$$w_i = b_i \exp(j\omega(t - q_x x - q_y y - q_z z)), i = x, y, z \quad (16)$$

In the above equations, a_i and b_i are the amplitude of displacement components, and t represents the time. Due to the considered assumption for wave propagation, u_y^s, w_y , the wavenumber component in the y -direction is zero. Hence, the displacement components can be obtained by solving a six-equation system, which is given as follows:

$$[\mathbf{A}]\{a_x \quad a_z \quad b_x \quad b_z\}^T = \{\mathbf{0}\} \quad (17)$$

$$[\mathbf{B}]\{a_y \quad b_y\}^T = \{\mathbf{0}\} \quad (18)$$

Substituting Equations (17) and (18) into Equations (9)-(14), $[\mathbf{A}]$ and $[\mathbf{B}]$ are calculated as follows:

$$[\mathbf{A}] = \begin{bmatrix} \rho - B_5 q_z^2 - (2B_1 + B_2)q_x^2 + D_1 & -q_x q_z (B_3 + B_5) & \rho_0 + B_6 q_x^2 + D_2 & B_6 q_x q_z \\ -q_x q_z (B_3 + B_5) & \rho - B_4 q_z^2 - B_5 q_x^2 + D_1 & B_7 q_x q_z & \rho_0 + B_7 q_z^2 + D_2 \\ \rho_0 + B_6 q_x^2 & B_7 q_x q_z & -B_8 q_x^2 + C_x & -B_8 q_x q_z \\ B_6 q_x q_z & \rho_0 + B_7 q_z^2 + D_3 & -B_8 q_x q_z & -B_8 q_z^2 + C_z + D_4 \end{bmatrix} \quad (19)$$

$$[\mathbf{B}] = \begin{bmatrix} \rho - B_5 q_z^2 - B_1 q_x^2 + D_1 & \rho_0 + D_2 \\ \rho_0 & C_y \end{bmatrix} \quad (20)$$

where the coefficients of D_1 to D_4 in terms of solid and fluid nonlocal parameters are defined by:

$$D_1 = \mu_s \rho \omega^2 (q_x^2 + q_z^2) \quad (21)$$

$$D_2 = \mu_s \rho_0 \omega^2 (q_x^2 + q_z^2) \quad (22)$$

$$D_3 = \mu_f \rho_0 \omega^2 (q_x^2 + q_z^2) \quad (23)$$

$$D_4 = \mu_f C_z \omega^2 (q_x^2 + q_z^2) \quad (24)$$

Here, the waves are polarized on the nanocomposite porous layer and perpendicular to it. The independence of a_y and b_y on a_x, a_z, b_x and b_z justifies the decoupling of slow waves polarized in the y -direction and the waves polarized in the meridian plane. If the square matrix determinant of Equation (19) equals zero, a nontrivial solution will exist to obtain the amplitude of displacement components. Hence, by calculating this determinant, a third-degree polynomial equation in terms of q_z^2 is obtained as follows:

$$V_0 q_z^6 + V_1 q_z^4 + V_2 q_z^3 + V_3 = 0 \quad (25)$$

The coefficients V_i can be calculated using computational software such as MATLAB or Maple. The six roots of q_z are obtained that $q_z(1), q_z(2)$ and $q_z(3)$ correspond to the three upgoing waves with the positive real parts and $q_z(4), q_z(5)$ and $q_z(6)$ are related to the three downgoing waves with negative real parts.

$$q_z(1) = -q_z(6), \quad q_z(2) = -q_z(5), \quad q_z(3) = -q_z(4) \quad (26)$$

Considering the first three equations of Equation (19), the amplitudes a_x, a_z, b_x and b_z can be calculated by using a normalized coefficient $N = a_z + b_z$ that is the displacement component amplitude $(1 - \phi)u_z^s + \phi u_z^f$ [31]. Thus, the amplitude of displacement components can be obtained by the following equation:

$$\begin{Bmatrix} a_x \\ a_z \\ b_x \end{Bmatrix} = \begin{bmatrix} A_{11} & A_{12} - A_{14} & A_{13} \\ A_{21} & A_{22} - A_{24} & A_{23} \\ A_{31} & A_{32} - A_{34} & A_{33} \end{bmatrix}^{-1} \begin{Bmatrix} -NA_{14} \\ -NA_{24} \\ -NA_{34} \end{Bmatrix}, \quad b_z = N - a_z \quad (27)$$

If the square matrix's determinant $[B]$ in Equation (20) is equal to zero, a nontrivial solution for polarized waves perpendicular to the xz -plane will exist. So, the value of q_z^2 is:

$$q_z^2 = \frac{\left(\rho - B_1 q_x^2 - \frac{\rho_0^2}{C_y} + \left(\mu_s \rho \omega^2 - \frac{\mu_s \rho_0^2 \omega^2}{C_y}\right) q_x^2\right)}{\left(B_5 - \mu_s \rho \omega^2 + \frac{\mu_s \rho_0^2 \omega^2}{C_y}\right)} \quad (28)$$

These waves should be normalized by $a_y = N$, such that:

$$b_y = -\frac{N\rho_0}{C_y} \quad (29)$$

By considering $N = 1$ and $q_z = \pm q_z(i), i = 1, 2, 3$, the amplitudes $a_x^\pm(i), a_z^\pm(i), b_x^\pm(i)$ and $b_z^\pm(i)$ are the solutions of Equation (27). Therefore, when $q_z(i) \rightarrow -q_z(i)$, N remains equal to one; consequently, one can write:

$$a_x^+ = -a_x^-, \quad a_z^+ = a_z^-, \quad b_x^+ = -b_x^-, \quad b_z^+ = b_z^- \quad (30)$$

The solid and fluid-discharge displacement components in the directions of x and z can be written as a sum of six waves [32] by defining the normalized factors $N(n)$

$$u_x^s = \sum_{n=1}^6 N(n) a_x(n) \exp(j\omega(t - q_x x - q_z(n)z)) \quad (31)$$

$$u_z^s = \sum_{n=1}^6 N(n) a_z(n) \exp(j\omega(t - q_x x - q_z(n)z)) \quad (32)$$

$$w_x = \sum_{n=1}^6 N(n) b_x(n) \exp(j\omega(t - q_x x - q_z(n)z)) \quad (33)$$

$$w_z = \sum_{n=1}^6 N(n)b_z(n) \exp(j\omega(t - q_x x - q_z(n)z)) \quad (34)$$

where $N(n)$ is the relative amplitude of the three reflected waves relative to the three absorbed waves. The following column states that a vector is used to describe the stress field, the displacement field, and the acoustic pressure as follows:

$$\mathbf{V}(z) = [u_x^s \quad u_z^s \quad w_z \quad \sigma_{zz}^t \quad \sigma_{xz}^t \quad p]^T \quad (35)$$

Moreover, the column vector \mathbf{N} is given by the following relation.

$$\mathbf{N} = [N_x^+ + N_x^- \quad N_x^+ - N_x^- \quad N_y^+ + N_y^- \quad N_y^+ - N_y^- \quad N_z^+ + N_z^- \quad N_z^+ - N_z^-]^T \quad (36)$$

where N_x^+, N_y^+ and N_z^+ are the normalization factors for the three waves are absorbed and N_x^-, N_y^- and N_z^- , for the three waves, are reflected. The state vector \mathbf{V} corresponds to the vector \mathbf{N} by

$$\mathbf{V}(z) = [\Gamma(z)]\mathbf{N} \quad (37)$$

thus, there is the following equation to correlate the vectors $\mathbf{V}(L)$ and $\mathbf{V}(0)$ to each other

$$\mathbf{V}(L) = [T]\mathbf{V}(0) \quad (38)$$

where L is the thickness of the nanocomposite porous layer. The transfer matrix elements for the porous layer are obtained by

$$[T] = [\Gamma(L)][\Gamma(0)]^{-1} \quad (39)$$

where the elements Γ_{mn} are calculated in terms of frequency by substituting the stress field, displacement field, and acoustic pressure into Equation (38) [31]. Figure 1 shows that the nanocomposite porous layer is connected to a rigid, impermeable backing. So, by considering the boundary conditions at $z = L$ and $z = 0$, one can write

$$\mathbf{V}(L) = [u_x^s(L) = 0 \quad u_z^s(L) = 0 \quad w_z(L) = 0 \quad \sigma_{zz}^t(L) \quad \sigma_{xz}^t(L) \quad p(L)]^T \quad (40)$$

$$\mathbf{V}(0) = [u_x^s(0) \quad u_z^s(0) \quad w_z(0) \quad \sigma_{zz}^t(0) = -p \quad \sigma_{xz}^t(0) = 0 \quad p(0) = p]^T \quad (41)$$

The surface impedance corresponds to the acoustic pressure and the z -component of air velocity. In addition, the air velocity is related to the solid phase and fluid-discharge displacements as follows:

$$p = Z_s v_z \quad (42)$$

$$v_z = (w_z + u_z)j\omega \quad (43)$$

Considering Equations (40-43), a three-equation system in terms of surface impedance is obtained.

$$T_{11}u_x^s + (T_{12} - T_{13})u_z^s + \left(\frac{T_{13}}{j\omega Z_s} - T_{14} + T_{16}\right)p = 0 \quad (44)$$

$$T_{21}u_x^s + (T_{22} - T_{23})u_z^s + \left(\frac{T_{23}}{j\omega Z_s} - T_{24} + T_{26}\right)p = 0 \tag{45}$$

$$T_{31}u_x^s + (T_{32} - T_{33})u_z^s + \left(\frac{T_{33}}{j\omega Z_s} - T_{34} + T_{36}\right)p = 0 \tag{46}$$

Hence, the surface impedance is obtained by using the Cramer rule as follows.

$$Z_s = -\frac{\Lambda_2}{j\omega\Lambda_1}, \Lambda_1 = \begin{vmatrix} T_{11} & T_{12} - T_{13} & T_{16} - T_{14} \\ T_{21} & T_{22} - T_{23} & T_{26} - T_{24} \\ T_{31} & T_{32} - T_{33} & T_{36} - T_{34} \end{vmatrix}, \Lambda_2 = \begin{vmatrix} T_{11} & T_{12} - T_{13} & T_{13} \\ T_{21} & T_{22} - T_{23} & T_{23} \\ T_{31} & T_{32} - T_{33} & T_{33} \end{vmatrix} \tag{47}$$

The acoustic performance of porous materials in wave propagation is characterized by the absorption coefficient α as follows

$$\alpha = 1 - |R|^2 \tag{48}$$

where R is the reflection coefficient in terms of the surface impedance Z_s and the characteristic impedance Z_0 .

$$R = \frac{Z_s - Z_0}{Z_s + Z_0}, Z_0 = \rho_0 c_0 = \sqrt{\rho_0 K_0} \tag{49}$$

In Equation (49) c_0 , ρ_0 and K_0 represent the sound speed, density, and bulk modulus of air, respectively. Consequently, the absorption coefficient can be computed using the transfer matrix method by solving the governing equations. The acoustic behavior of the nanocomposite porous layer can be described in normal wave propagation [31].

4. Experiments

The details of the materials used and the procedure for fabricating samples are presented in Refs. [5, 33]. The considered multi-walled carbon nanotubes (MWCNTs) in this research are four different samples, one of which is unfunctionalized. The other three samples are functionalized with diameters of 5-15nm, 20-30nm, and 50-80nm. Additionally, the composition and part-by-weight percent of constituents are presented in Table 1. Different instruments and standards have been used to characterize and measure the properties as mentioned in Ref. [5].

Table 1. Composition and part by weight of reactants for producing neat PU foams.

	Polyol	Isocyanate	Distilled water	Amine catalyst	Silicone surfactant	Tin catalyst	Physical blowing agent	Glycerin
Part by weight	100	85.38	7	1.5	1.5	0.25	8	3.5

5. Measurement and characterization of mechanical, acoustic, and non-acoustical properties

Direct laboratory methods can measure all mechanical properties and non-acoustical characteristics of produced foams. Few laboratory methods exist for non-acoustical characteristics such as tortuosity, thermal, and viscosity characteristic lengths; however, these methods are not easily available. In many studies, these parameters are predicted using semi-empirical methods such as scanning electron microscopy (SEM) or indirect methods. In this study, the indirect method is used to predict these parameters.

5.1 Mechanical and structural properties of produced samples

Table 2 shows various mechanical and structural characteristics of the produced foam nanocomposite samples. The structural properties are measured according to the ISO 3386 standard, and the density is determined using the ASTM D3574 standard in a laboratory, utilizing a large number of samples.

Table 2. Mechanical and structural characteristics of the produced nanocomposite samples with different MWCNT.

Samples	Young modulus E(Pa)	Poison ratio ν	Structural damping η	Density $\frac{\rho_1(\text{kg})}{\text{m}^3}$
Nanocyl nanocomposite sample	27884.47 ± 5579.12	0.47 ± 0.01	0.0846 ± 0.0025	26.31 ± 1.27
PU/CNT functionalized nanocomposite with a diameter of 5-15 nm	97263.43 ± 13147.91	0.41 ± 0.02	0.0918 ± 0.0031	26.72 ± 1.08
PU/CNT functionalized nanocomposite with a diameter of 20-30 nm	73796.62 ± 10302.28	0.43 ± 0.12	0.0938 ± 0.0035	27.02 ± 1.17
PU/CNT functionalized nanocomposite with a diameter of 50-80 nm	63144.61 ± 5158.66	0.47 ± 0.08	0.0954 ± 0.0078	31.49 ± 1.01

5.2 Non-Acoustical Properties of Produced Samples: Indirect Methods

In the analysis of the behavior of porous materials, it has always been challenging to calculate three non-acoustic parameters, including the characteristic length of torsion, thermal properties, and viscosity. One method for calculating these three parameters is the indirect calculation method. The method used in this study is strictly compatible with the process presented in [33]. It is noteworthy that the equations used in this research are the modified Biot equations.

Table 3. Comparison between the non-acoustical characteristics of the produced nanocomposite samples.

Samples	Porosity ϕ	Flow resistivity $\sigma\left(\frac{Ns}{m^2}\right)$	Tortuosity α_∞	Thermal typical length Λ' (μm)	Viscous characteristic length Λ (μm)
Nanocomposite foam by Nanocyl MWCNT ($\frac{l}{d} = 158$)	97.4807 \pm 0.8598	5716.84 \pm 740.44	2.6578 \pm 0.1929	166.3184 \pm 20.022	54.8575 \pm 1.8184
Nanocomposite foam by functionalized MWCNT with O.D. 5-15 nm ($\frac{l}{d} = 5000$)	91.2111 \pm 1.9134	4985.664 \pm 530.81	2.1439 \pm 0.2211	171.9391 \pm 13.876	47.6531 \pm 6.1401
Nanocomposite foam by functionalized MWCNT with O.D. 20-30 nm ($\frac{l}{d} = 800$)	94.2875 \pm 0.8886	5014.209 \pm 536.24	1.4309 \pm 0.1839	182.5217 \pm 22.293	24.6946 \pm 4.6624
Nanocomposite foam by functionalized MWCNT with O.D. 50-80 nm ($\frac{l}{d} = 230$)	91.824 \pm 1.0469	5241.960 \pm 223.76	1.2390 \pm 0.0912	183.8538 \pm 23.9464	38.9581 \pm 18.7346

Based on the indirect method, the three features are calculated separately for each sample. The presented process for samples 2 and 3 cm thick, is based on the statistical methods for each set. Many samples are calculated, and the non-acoustical characteristics of the produced nanocomposite samples are presented in Table 3. The presented results are the statistical analysis of data from different samples. Figure 2 shows the SEM images of all nanocomposite samples, which are used to determine their porosity.

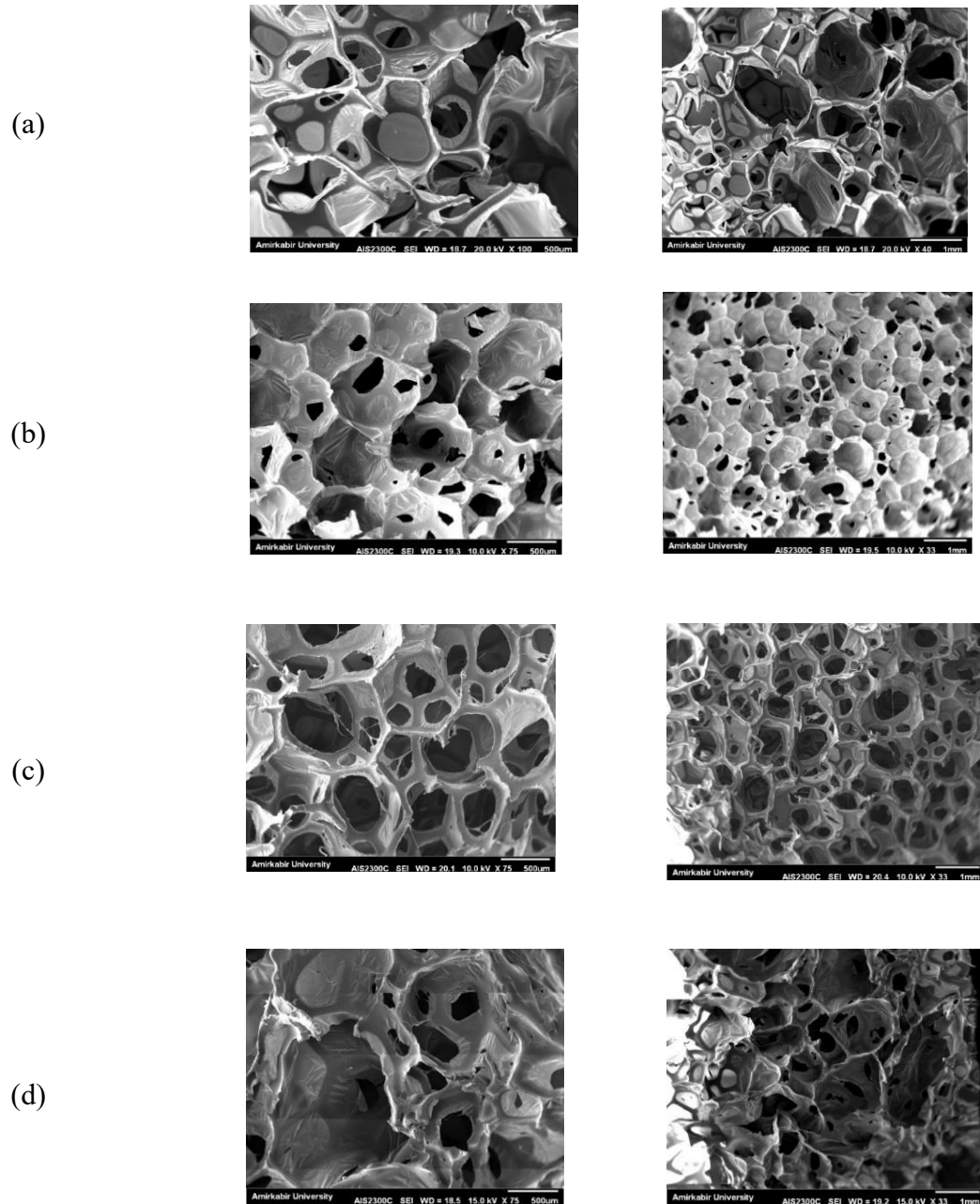


Fig.2. SEM images from a) nanocomposite foam by Nanocyl MWCNT ($\frac{l}{d} = 158$); b) nanocomposite foam by functionalized MWCNT with O.D. 50 to 80 nm ($\frac{l}{d} = 230$); c) nanocomposite foam by functionalized MWCNT with O.D. 20 to 30 nm ($\frac{l}{d} = 800$); d) nanocomposite foam by functionalized MWCNT with O.D. 5 to 15 nm ($\frac{l}{d} = 5000$).

6. Results and discussion

6.1 Model verification

This section verifies the theoretical results in this paper with previous work. The absorption coefficient of a nanocomposite porous foam with mechanical, acoustic, and non-acoustic properties as presented in [20] is calculated based on the modified Biot theory using the updated transfer matrix method and compared with the corresponding reference results. As shown in Figure 3, the present study predicts the same results as those of Hasani Baferani and Ohadi [20], indicating the correct performance of the updated transfer matrix method.

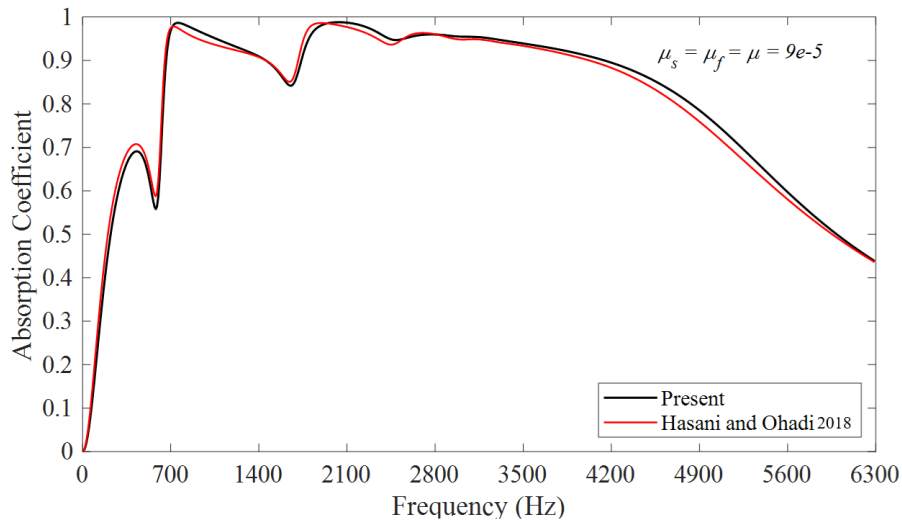


Fig.3. Comparison between the absorption coefficient of a nanocomposite porous foam based on modified Biot's theory versus frequency, calculated by the transfer matrix method with ref [20].

6.2. Comparison of models by experimental samples

In the following, the experimental results obtained from the impedance tube test will be compared with the predicted results based on Biot's theory and Biot's modified theory for different nanocomposite samples produced. Mechanical and non-acoustic properties are used based on the results presented in Table 3.

6.2.1. Nanocomposite foams by Nanocyl MWCNT

In this subsection, the experimental results of the acoustic absorption coefficient are compared with the corresponding results of the absorption coefficient based on Biot's theory ($\mu_s = \mu_f = 0$) and modified Biot's theory ($\mu_s > 0, \mu_f \geq 0$) for different values of solid and fluid phase nonlocal parameters. Figures 4 and 5 show the comparison between the experimental results and the theoretical predictions based on Biot's and modified Biot's theories in the condition of including the fluid non-local effect for the Nanocyl MWCNT nanocomposite sample with a thickness of 2 cm in the frequency range from 0 to 1000 Hz (Figure 4) and 0 to 6300 Hz (Figure 5). As can be seen, in the low-frequency range (0 to 1000 Hz), for small values of solid and fluid nonlocal

parameters, the modified Biot and Biot theories yield the same sound absorption results. Still, in this frequency range, the experimental results differ somewhat from the theoretical results (Figure 4a).

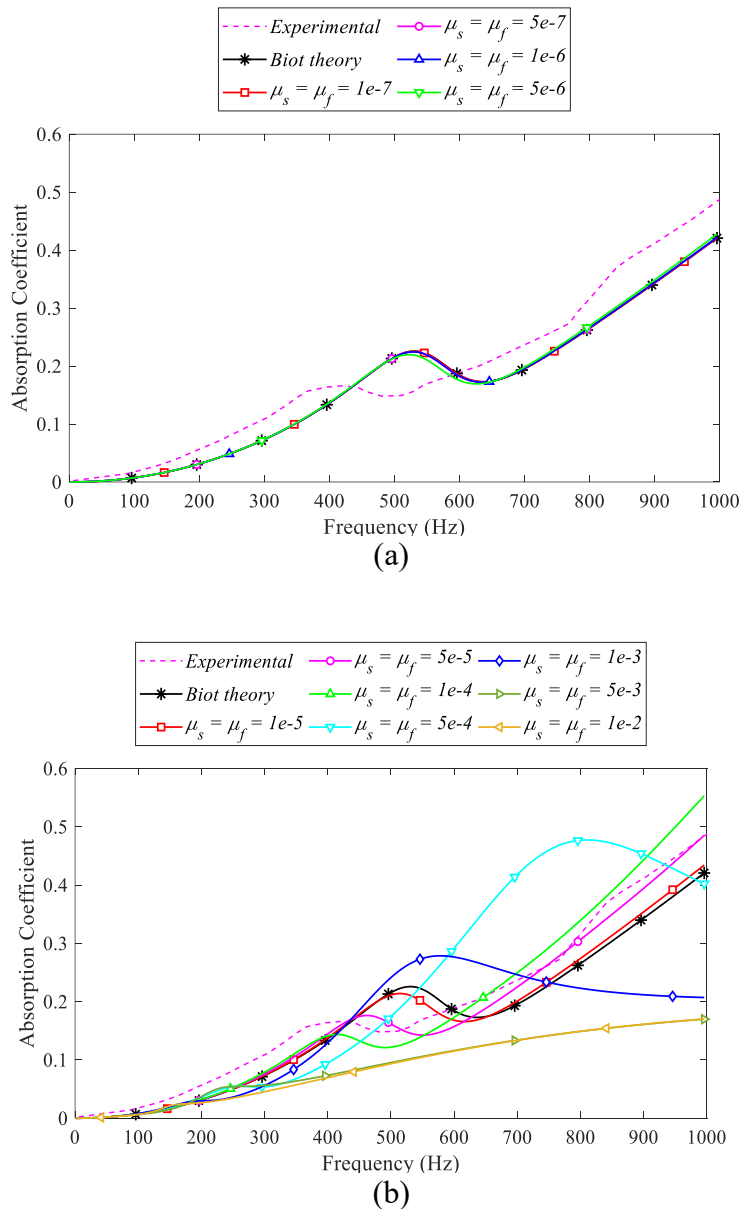


Fig. 4. Comparison between the experimental results and the predicted results based on Biot's and modified Biot's theories for nanocomposite foam by Nanocyl MWCNT with 2 cm thickness in the situation of including fluid nonlocal effect; a) $1e-7 \leq \mu_s = \mu_f \leq 5e-6$, b) $1e-5 \leq \mu_s = \mu_f \leq 1e-2$.

By increasing the values of nonlocal parameters in the low-frequency range, Biot's and modified Biot's theories predict different results; however, modified Biot's theory and experimental results have a good agreement considering $\mu_s = \mu_f = 1e-4$. The results obtained by modified Biot's theory differ from Biot's theory, especially since these results are more remarkable than those for $\mu_s = \mu_f > 1e-4$ (Figure 4b). The theoretical models still predict similar results by increasing the

frequency to the range of 6300 Hz and considering the small values of the solid and fluid nonlocal parameters. The results of modified Biot's theory agree with the experimental results for $\mu_s = \mu_f = 5e^{-6}$ (Figure 5a). The absorption coefficients predicted by the modified Biot theory decrease at high-frequency ranges for the values of nonlocal parameters $\mu_s = \mu_f > 5e^{-6}$ and move away from the Biot theory and experimental results. Considering the larger values of the nonlocal parameter for solid and fluid phases, modified Biot's theory and experimental results do not match (Figure 5b).

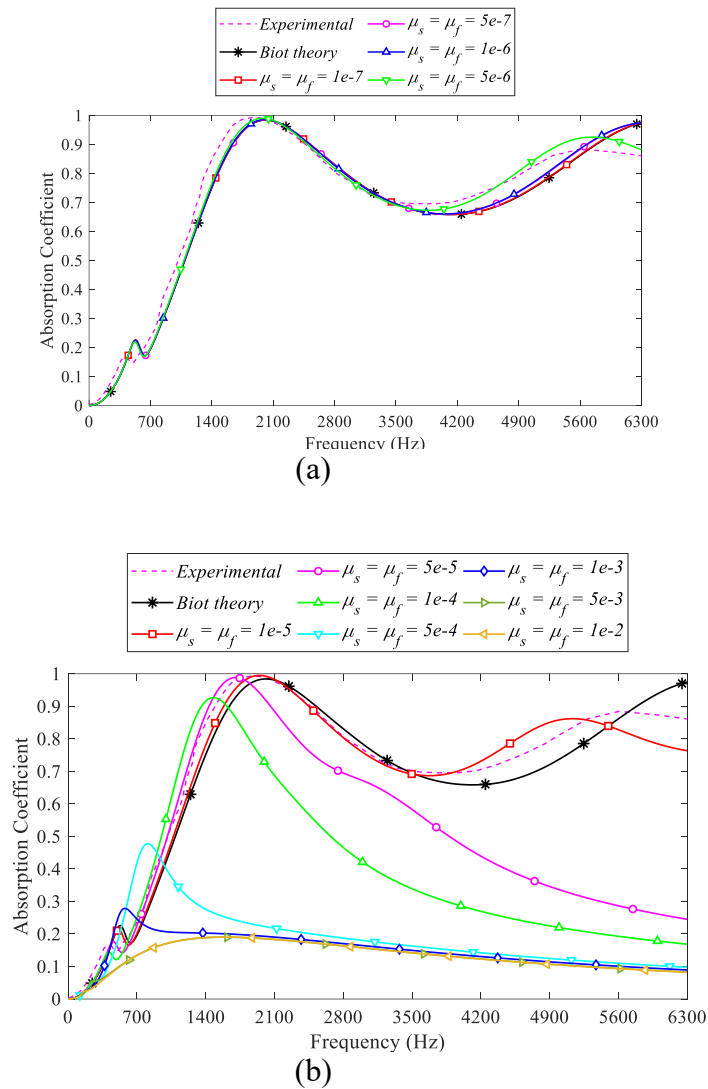


Fig.5. Comparison between the experimental results and the predicted results based on Biot's and modified Biot's theories for nanocomposite foam by Nanocyl MWCNT with 2 cm thickness versus frequency in the situation of including fluid nonlocal effect; a) $1e - 7 \leq \mu_s = \mu_f \leq 5e - 6$, b) $1e - 5 \leq \mu_s = \mu_f \leq 1e - 2$.

In Figure 6, the variation of the absorption coefficient of this foam is presented only considering the nonlocal coefficient on the solid phase. As can be seen, the results presented by modified Biot's theory have a much better approximation than Biot's theory, especially when the fluid nonlocal

effect is ignored ($\mu_f = 0$). In the first situation (including the fluid nonlocal effect), when the nonlocal parameters for both phases are increased, the foam's absorption coefficient decreases, which is far from the experimental results. In this situation, the theoretical and experimental results for $\mu_s = \mu_f = 5e - 6$ have a good agreement.

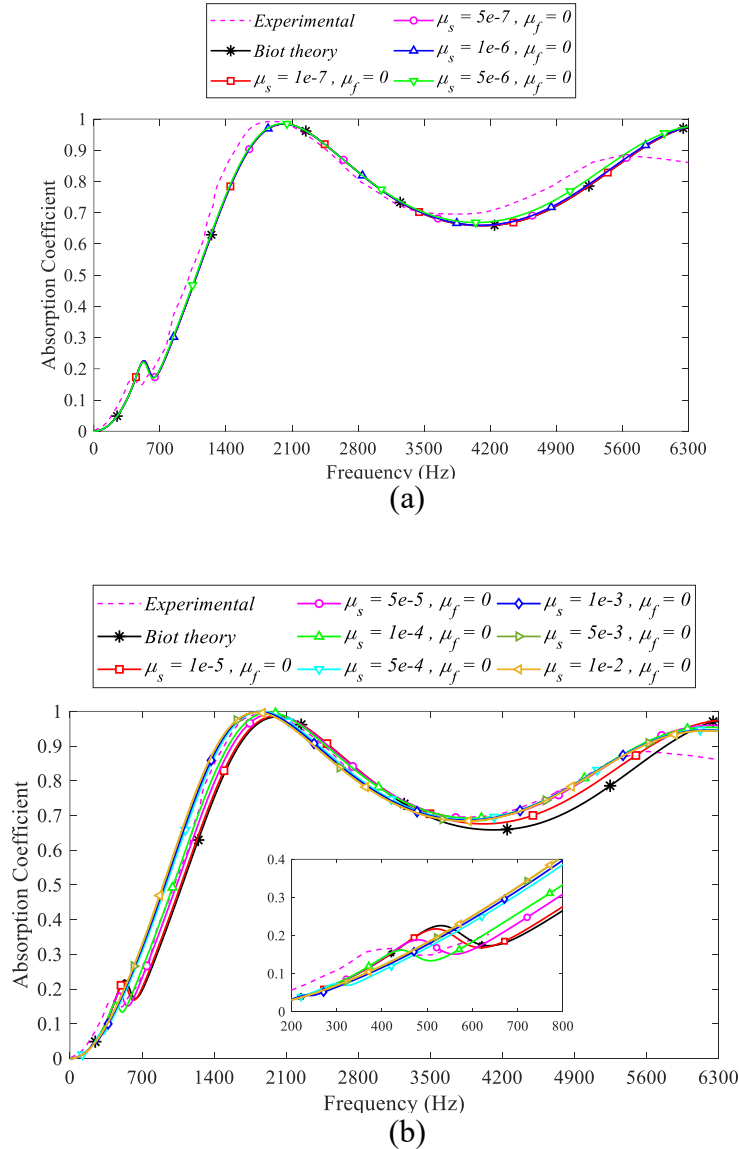


Fig.6. Comparison between the experimental results and the predicted results based on Biot's and modified Biot's theories for nanocomposite foam by Nanocyl MWCNT with 2 cm thickness versus frequency in the situation of excluding fluid nonlocal effect; a) $1e - 7 \leq \mu_s \leq 5e - 6, \mu_f = 0$, b) $1e - 5 \leq \mu_s \leq 1e - 2, \mu_f = 0$.

In contrast, the theoretical results are closer to experimental results in the second situation (excluding the fluid nonlocal effect). The model becomes more accurate as the solid nonlocal parameter is increased. It is necessary to note that the non-acoustical properties used in modified

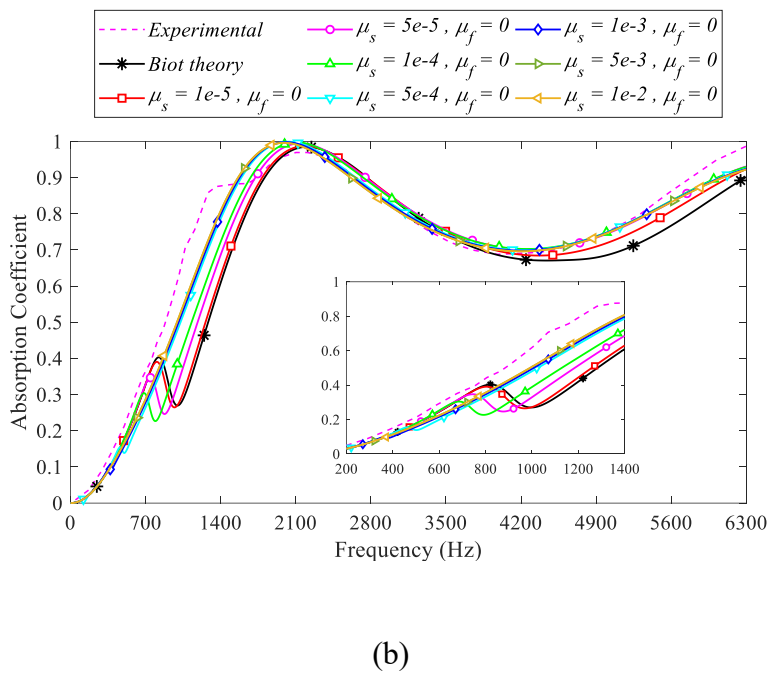
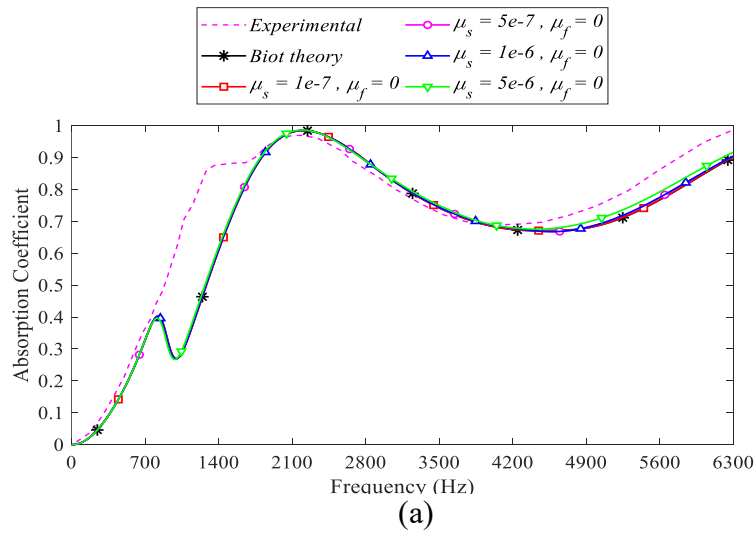


Fig.7. Comparison between the experimental results and the predicted results based on Biot's and modified Biot's theories for nanocomposite foam by functionalized MWCNT with O.D. 5 to 15 nm and 2 cm thickness versus frequency in the situation of excluding fluid nonlocal effect; a) $1e - 7 \leq \mu_s \leq 5e - 6, \mu_f = 0$, b) $1e - 5 \leq \mu_s \leq 1e - 2, \mu_f = 0$.

Biot's theory are based on the information presented in Table 3, which is derived from an indirect statistical method using at least 40 different samples of Biot's theory. It can be concluded from the presented results in Figures 4 and 5 that modified Biot's and Biot's theories provide a good approxi-

mation of the behavior of nanocomposite porous materials. Specifically, behavioral predictability is better when the fluid nonlocal effect is ignored. As shown in Figure 6, the best agreement between the modified Biot's theory and the experimental results is when $\mu_s = 1e - 4, \mu_f = 0$ at the frequency range from 0 to 5400 Hz.

Since the obtained theoretical results in the second situation (excluding the fluid nonlocal effect) for this foam were in better agreement with experimental results, only the other foams' predicted results from the second situation are presented.

6.2.2. Nanocomposite Foam by functionalized MWCNT with O. D. 5-15 nm

This subsection presents the variation of the absorption coefficient for nanocomposite foam samples functionalized with MWCNT with diameters ranging from 5 to 15 nm. Figure 7 compares the variations of Biot's absorption coefficient predictions and modified Biot's theories with experimental results as a function of frequency. As seen, Biot's and modified Biot's theories can predict the behavior of nanocomposite samples with excellent approximation, especially when the nonlocal parameter of the solid phase is increased. Modified Biot's theory can better approximate the behavior of nanocomposite foams. The best agreement between the results predicted by modified Biot's theory and the experimental results is when $\mu_s = 1e - 3, \mu_f = 0$. There is a significant difference between the theoretical and experimental results at low frequencies for $\mu_s < 1e - 3, \mu_f = 0$. Simultaneously when $\mu_s \geq 1e - 3, \mu_f = 0$, a good agreement is observed between the experimental results and theoretical predictions from modified Biot's theory at the low and high-frequency ranges. Hence, it can be concluded that the modified Biot's theory can predict the acoustic performance of these materials more accurately than Biot's theory in the frequency range from 0 to 5300 Hz.

6.2.3. Nanocomposite foam by functionalized MWCNT with O. D. 20-30 nm

This subsection illustrates the behavior of the absorption coefficient of different samples of the produced nanocomposite foam with an O.D. of 20-30 nm. MWCNT is compared with the results predicted by Biot's and modified Biot's theories with a thickness of 2 cm. The absorption coefficients of nanocomposite foam by functionalized MWCNT with O.D. 20 to 30 nm are shown in Figure 8, predicted by the mentioned theories, excluding the nonlocal parameter fluid phase, with experimental results. In this foam, by excluding the nonlocal effects of the fluid phase and considering the value of the solid nonlocal parameter $\mu_s = 5e - 4$, there is a good agreement between the theoretical predictions and experimental results in the range of frequency from 0 to 3500 Hz. Larger values of the solid nonlocal parameter ($\mu_s > 5e - 4$) do not change the theoretical, but smaller values ($\mu_s < 5e - 4$), bring the results closer to the Biot theory and deviate from laboratory results.

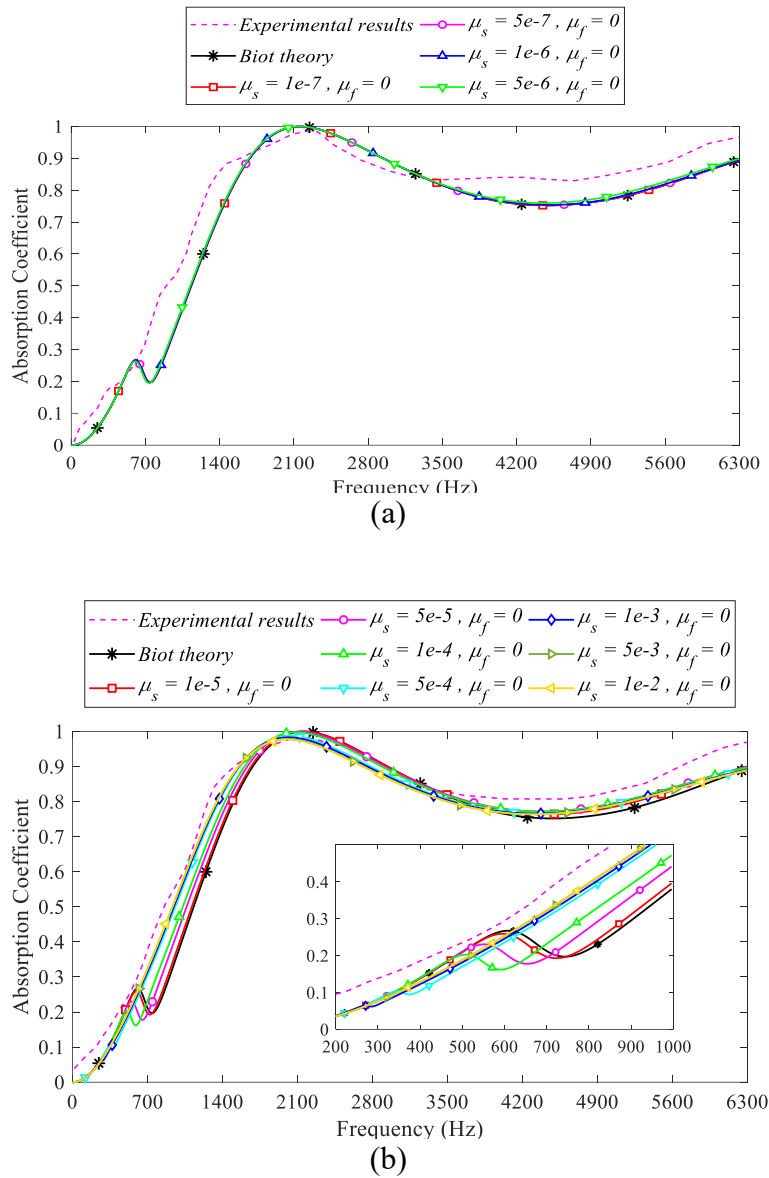


Fig.8. Comparison between the experimental results and the predicted results based on Biot's and modified Biot's theories for nanocomposite foam by functionalized MWCNT with O.D. 20 to 30 nm and 2 cm thickness versus frequency in the situation of excluding fluid nonlocal effect; a) $1e-7 \leq \mu_s \leq 5e-6, \mu_f = 0$, b) $1e-5 \leq \mu_s \leq 1e-2, \mu_f = 0$.

6.2.4. Nanocomposite foam by functionalized MWCNT with O. D. 50-80 nm

In this subsection, the acoustic absorption coefficient of a nanocomposite sample with functionalized MWCNTs with an outer diameter of 50-80 nm and 2 cm thickness has been investigated in Figure 9. Similar to previous observations, there is a good agreement between the experimental and theoretical results for large values of solid nonlocal parameters, especially in the low-frequency range when the solid nonlocal parameter is $\mu_s = 1e-3$ and the fluid nonlocal

parameter is zero. For values higher than $1e - 3$, the theoretical results do not change significantly, but for smaller values, the results approach Biot's theory in a frequency range from 0 to 4500.

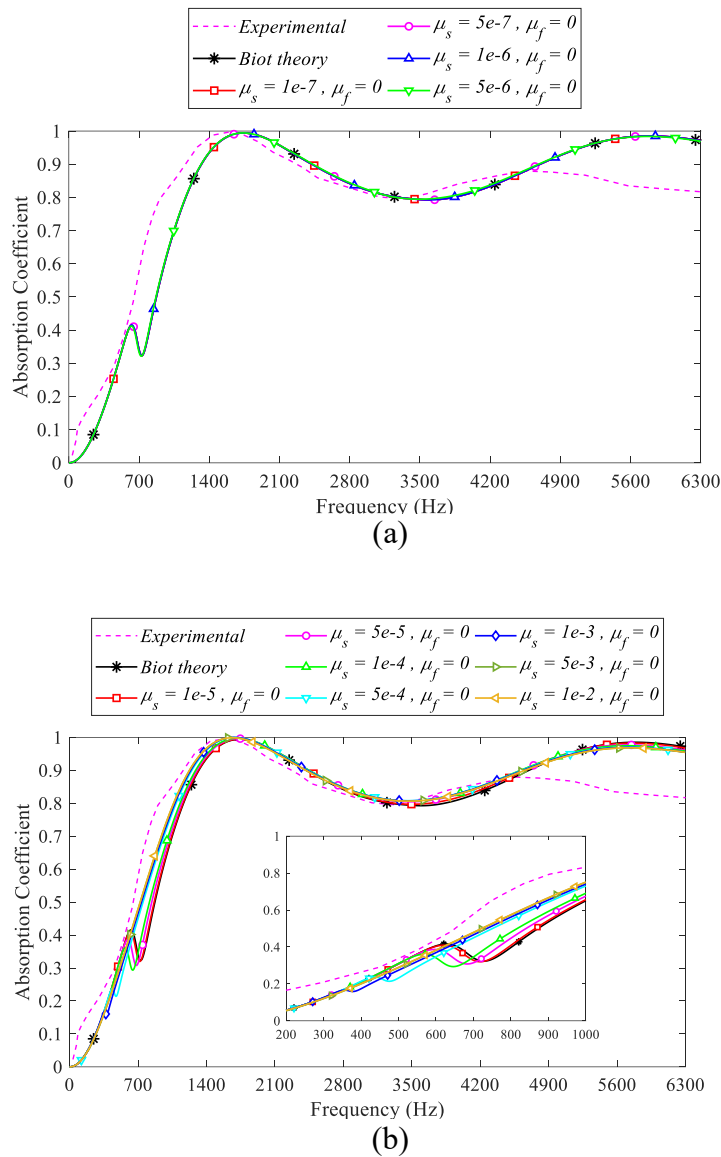


Fig. 9. Comparison between the experimental results and the predicted results based on Biot's and modified Biot's theories for nanocomposite foam by functionalized MWCNT with O.D. 50 to 80 nm and 2 cm thickness versus frequency in the situation of excluding fluid nonlocal effect; a) $1e - 7 \leq \mu_s \leq 5e - 6, \mu_f = 0$, b) $1e - 5 \leq \mu_s \leq 1e - 2, \mu_f = 0$.

6. Conclusions

This paper presents wave propagation in nanocomposite porous materials based on the modified Biot's theory. The governing equations were solved for the first time using the transfer matrix method. Subsequently, several nanocomposite foams with different multiwall carbon nanotubes were produced. Eventually, a comparison was presented between Biot's predicted results and

modified Biot's equations in two situations: one including and the other excluding the nonlocal effect of the fluid phase, along with experimental results. The findings are summarized as:

Biot's and modified Biot's equations have predicted the changes in the acoustic absorption coefficient of produced nanocomposite foams with an acceptable approximation.

In the first situation (including the fluid nonlocal effect), the modified Biot's theory's predicted results are similar to those of Biot's theory, with approximately the same values in the low-frequency range for different nonlocal parameter values.

The absorption coefficient also decreases as the nonlocal parameters of the solid and fluid phases decrease in a high-frequency range. It tends to zero for large values of nonlocal parameters of the solid and fluid phases.

Notably, there is a significant difference between Biot's and modified Biot's theories for different values of the solid nonlocal parameter in high-frequency ranges.

By comparing the results predicted by the modified Biot theory with the experimental results for the nanocomposite porous materials investigated in this paper, it can be seen that models excluding the fluid nonlocal effect for significant solid nonlocal parameters are more suitable for predicting wave characteristics in nanocomposite porous materials.

Increasing the solid nonlocal parameter μ_s , the highest degree of overlap with experimental results is obtained in all produced nanocomposite foams for a large part of the frequency range.

References

- [1] F. Fraternali, T. Blesgen, A. Amendola, C. Daraio, Multiscale mass-spring models of carbon nanotube foams, *Journal of the Mechanics and Physics of Solids*, 59 (2011) 89-102.
- [2] E. Ogam, Z.E.A. Fella, G. Ogam, Identification of the mechanical moduli of closed-cell porous foams using transmitted acoustic waves in air and the transfer matrix method, *Composite structures*, 135 (2016) 205-216.
- [3] J. Wang, S. Fang, State space solution of non-axisymmetric Biot consolidation problem for multilayered porous media, *International Journal of Engineering Science*, 41 (2003) 1799-1813.
- [4] L. Zhang, E.D. Yilmaz, J. Schjødt-Thomsen, J.C. Rauhe, R. Pyrz, MWNT reinforced polyurethane foam: Processing, characterization and modelling of mechanical properties, *Composites Science and Technology*, 71 (2011) 877-884.
- [5] A.H. Baferani, A. Katbab, A. Ohadi, The role of sonication time upon acoustic wave absorption efficiency, microstructure, and viscoelastic behavior of flexible polyurethane/CNT nanocomposite foam, *European Polymer Journal*, 90 (2017) 383-391.
- [6] M. Bandarian, A. Shojaei, A.M. Rashidi, Thermal, mechanical and acoustic damping properties of flexible open-cell polyurethane/multi-walled carbon nanotube foams: effect of surface functionality of nanotubes, *Polymer International*, 60 (2011) 475-482.
- [7] Z.C. Lee LJ, Cao X, et al. , Polymer nanocomposite foams, *Composites Science and Technology*, (2005).

- [8] O. Smorygo, V. Mikutski, A. Marukovich, V. Sadykov, Y. Bospalko, A. Stefan, C.-E. Pelin, Preparation and characterization of open-cell epoxy foams modified with carbon fibers and aluminum powder, *Composite Structures*, 202 (2018) 917-923.
- [9] R. Verdejo, R. Stämpfli, M. Alvarez-Lainez, S. Mourad, M. Rodriguez-Perez, P. Brühwiler, M. Shaffer, Enhanced acoustic damping in flexible polyurethane foams filled with carbon nanotubes, *Composites Science and Technology*, 69 (2009) 1564-1569.
- [10] A.M. Willemsen, M.D. Rao, Sound absorption characteristics of nanocomposite polyurethane foams infused with carbon nanotubes, *Noise Control Engineering Journal*, 63 (2015) 424-438.
- [11] A.C. Eringen, Nonlocal polar elastic continua, *International journal of engineering science*, 10 (1972) 1-16.
- [12] A.C. Eringen, D. Edelen, On nonlocal elasticity, *International journal of engineering science*, 10 (1972) 233-248.
- [13] A. Eringen, *Nonlocal polar field models*, New York: Academic, (1976).
- [14] A. Eringen, J. Wegner, Nonlocal continuum field theories, in, *American Society of Mechanical Engineers Digital Collection*, 2003.
- [15] A.C. Eringen, Linear theory of nonlocal elasticity and dispersion of plane waves, *International Journal of Engineering Science*, 10 (1972) 425-435.
- [16] A.C. Eringen, On differential equations of nonlocal elasticity and solutions of screw dislocation and surface waves, in, 1983.
- [17] A.C. Eringen, Theory of nonlocal elasticity and some applications, in, 1984.
- [18] A. Chakraborty, Prediction of negative dispersion by a nonlocal poroelastic theory, *The Journal of the Acoustical Society of America*, 123 (2008) 56-67.
- [19] L. Tong, Y. Yu, W. Hu, Y. Shi, C. Xu, On wave propagation characteristics in fluid saturated porous materials by a nonlocal Biot theory, *Journal of Sound and Vibration*, 379 (2016) 106-118.
- [20] A. Hasani Baferani, A. Ohadi, Analytical investigation of the acoustic behavior of nanocomposite porous media by using modified nonlocal Biot's equations, *Journal of Vibration and Control*, 24 (2018) 2701-2716.
- [21] L. Tong, S. Lai, L. Zeng, C. Xu, J. Yang, Nonlocal scale effect on Rayleigh wave propagation in porous fluid-saturated materials, *International Journal of Mechanical Sciences*, 148 (2018) 459-466.
- [22] L. Tong, L. Zeng, D. Geng, W. Hu, C. Xu, Dynamic effect of a moving ring load on a cylindrical structure embedded in poroelastic space based on nonlocal Biot theory, *Soil Dynamics and Earthquake Engineering*, 128 (2020) 105897.
- [23] S. Menon, X. Song, A stabilized computational nonlocal poromechanics model for dynamic analysis of saturated porous media, *International Journal for Numerical Methods in Engineering*, 122 (2021) 5512-5539.
- [24] H. Ding, S. Xu, C. Xu, L. Tong, Y. Jiang, Z. Lei, Influence factors on the nonlocal parameter and scale factor in strain gradient nonlocal Biot theory, *Soil Dynamics and Earthquake Engineering*, 166 (2023) 107779.
- [25] S. Xenos, Porous materials: constitutive modeling and computational issues, in, *Institut Polytechnique de Paris; Université de Thessalie*, 2024.

- [26] B. Ma, Theory of propagation of elastic waves in a fluid-saturated porous solid: I. Low-frequency range, *J Acoust Soc Am*, 28 (1956) 168-178.
- [27] M.A. Biot, Generalized theory of acoustic propagation in porous dissipative media, *The Journal of the Acoustical Society of America*, 34 (1962) 1254-1264.
- [28] J. Allard, N. Atalla, *Propagation of sound in porous media: modelling sound absorbing materials*, John Wiley & Sons, 2009.
- [29] D.L. Johnson, J. Koplik, R. Dashen, Theory of dynamic permeability and tortuosity in fluid-saturated porous media, *Journal of fluid mechanics*, 176 (1987) 379-402.
- [30] Y. Champoux, J.F. Allard, Dynamic tortuosity and bulk modulus in air-saturated porous media, *Journal of applied physics*, 70 (1991) 1975-1979.
- [31] A.K. Vashishth, P. Khurana, Waves in stratified anisotropic poroelastic media: a transfer matrix approach, *Journal of sound and vibration*, 277 (2004) 239-275.
- [32] A. Hasani Baferani, A. Ohadi, R. Keshavarz, Toward mechanistic understanding of the relationship between the sound absorption and the natural and resonant frequencies of porous media, *The Journal of the Acoustical Society of America*, 140 (2016) 4246-4259.
- [33] A.H. Baferani, R. Keshavarz, M. Asadi, A. Ohadi, Effects of Silicone Surfactant on the Properties of Open-Cell Flexible Polyurethane Foams, *Advances in Polymer Technology*, 37 (2018) 71-83.